The Chodura sheath for angles of a few degrees between the magnetic field and the surface of divertor targets and limiters

2012 Nucl. Fusion 52 083012

(http://iopscience.iop.org/0029-5515/52/8/083012)

IOP Publishing and International Atomic Energy Agency Nuclear Fusion
Nucl. Fusion **52** (2012) 083012 (10pp) doi:10.1088/0029-5515/52/8/083012

The Chodura sheath for angles of a few degrees between the magnetic field and the surface of divertor targets and limiters

P.C. Stangeby

University of Toronto Institute for Aerospace Studies, Toronto, Canada
and
DIII-D National Fusion Facility, San Diego, CA, USA

Received 9 January 2012, accepted for publication 21 June 2012
Published 11 July 2012
Online at stacks.iop.org/NF/52/083012

Abstract
To achieve low deposited power flux density to solid surfaces in magnetic fusion devices, very small values of α are required, where α is the angle between $\boldsymbol{B}$ and the surface tangent. For an oblique magnetic field, there exists in front of the solid surface a Chodura sheath (CS) (also known as the 'magnetic pre-sheath') of thickness several ρ_i, the ion Larmor radius. The standard assumption is that the CS is additional to the Debye sheath (DS) of thickness several λ_D, the Debye length. Simple fluid modelling for collisionless CS conditions gives the drop in normalized electrostatic potential across the CS as $e\Delta\phi_{CS}/kT_e = \ln(\sin\alpha)$. For an electrically floating wall there is the separate constraint of ambipolar flow to the wall $e\Delta\phi_{floating}/kT_e = 0.5\ln[(2\pi m_e/m_i)(1 + T_i/T_e)]$, where $\Delta\phi_{floating} = \Delta\phi_{CS} + \Delta\phi_{DS}$. For the case of a deuterium plasma and $T_i = T_e$, $|e\Delta\phi_{floating}/kT_e| = 2.84$. For $\alpha < 3.35^\circ$, $|e\Delta\phi_{CS}/kT_e|$ exceeds 2.84 which evidently implies that the DS ceases to exist for such values of α and the entire potential drop would then occur across the CS. New analysis of the CS provides solutions for a number of quantities of practical importance, which improve on the solutions presently in use in models and edge impurity codes. Compared with the latter, the results of the present analysis indicate that (i) the E-field directed towards the solid surface is stronger and (ii) the plasma density drops more rapidly approaching the solid surface. The effect of (i) is to increase the probability of prompt local deposition of sputtered particles, while (ii) has the opposite effect.

1. Introduction

Materials issues are often paramount in applications of science and it is recognized that this is likely to be the case for fusion energy as well, see for example the 'Greenwald Report' and the challenge of 'taming the plasma material interface' [1]. One of the principal materials challenges for magnetic fusion energy is the damage caused to plasma-facing components by energetic ions, electrons, photons and charge-exchange neutrals escaping the plasma. Virtually every aspect of the actual plasma (i.e. ion and electron) material interaction is controlled by the properties of the Debye sheath (DS) and Chodura sheath (CS) which separate the plasma and the solid material. It is therefore important that we have as correct as possible a description of these sheaths.

In the absence of a magnetic field, a positive space-charge layer—the DS—arises between the plasma and a solid object (herein referred to generically as 'the wall') in contact with the plasma. In the presence of a magnetic field, where the field lines are at angle $\alpha \neq 90^\circ$ to the tangent to the wall surface, an additional sheath arises—the magnetic pre-sheath or CS—located between the plasma and the DS [2]. Although the CS is quasi-neutral, it contains a strong E-field normal to the wall surface which turns the ion flow from being sonic/supersonic in the parallel-to-$\boldsymbol{B}$ direction at the entrance to the CS (which is the Chodura condition), to being sonic/supersonic in the perpendicular-to-wall direction at the exit from the CS i.e. at the entrance to the DS (which is the Bohm condition). For further discussion, see reference [3] and references therein.

The total drop in the electrostatic potential within the CS that is required to turn the ion flow direction depends on angle α, namely $e\Delta\phi_{CS}/kT_e = \ln(\sin\alpha)$ [2–4]. It is readily seen that as $\alpha \to 0$, $\Delta\phi_{CS} \to \infty$. This raises an apparent problem. For the most basic situation where the wall is electrically floating, the *total* drop in electrostatic potential between the plasma (i.e. upstream of the CS entrance) and the wall is finite. That is, the total potential drop across the combined CS and DS is finite and, assuming a monotonic spatial variation of potential throughout, this means that $\Delta\phi_{CS}$ must be finite. In fact, Chodura has shown [2] that for a floating surface the total potential drop across the combined sheaths is independent of α and is equal to the standard value, i.e. for non-magnetic

plasmas:

$$\frac{e\Delta\phi_{\text{floating}}}{kT_e} = \frac{e\Delta\phi_{CS} + e\Delta\phi_{DS}}{kT_e} = 0.51 \ln\left[\left(\frac{2\pi m_e}{m_i}\right)\left(1 + \frac{T_i}{T_e}\right)\right],$$

see [3] (the α-independence is exact for the simplest model of the CS but is only approximate for more sophisticated models, as discussed below).

The central point of this paper is that these two fundamental requirements for $\Delta\phi_{CS}$ and $\Delta\phi_{\text{floating}}$ are incompatible for small α. For example, for the case of a deuterium plasma and $T_i = T_e$, one finds $|e\Delta\phi_{\text{floating}}/kT_e| = 2.84$. For $\alpha < 3.35^\circ$, $|e\Delta\phi_{CS}/kT_e|$ exceeds 2.84 which evidently implies that the DS ceases to exist for such values of α. Chodura does not include such small angles in most of his figures and this situation appears not to have been discussed to date in the literature. Just such small angles, however, are of central interest for magnetic fusion devices, which generally employ angles of $\alpha \sim$ a few degrees, in order to reduce the deposited power flux density on solid surfaces.

This work addresses this issue by presenting a new model for the sheath for small angles α. The principal hypothesis here is that for sufficiently small angles the DS disappears and only a CS exists. It is found that the electric field in the CS is no longer strong enough to turn (the guiding centres of the) ions so that they are normal to the solid surface as they strike the solid surface, which otherwise happens in the CS. This, together with other changes to the sheath, have implications for a number of matters of practical interest, including the transport of sputtered of impurities, which are discussed.

The combined DS and CS control the relation between the plasma conditions near the solid surface (density and temperature) and plasma interaction with the solid surface, including not only the power deposition but also sputtering of the wall material by the impact of ions which gained much of their energy in falling through the combined sheath potential drop. In addition, the transport of the sputtered impurity particles, once they are ionized, in the near-surface region can be strongly influenced by the strong E-field and fast plasma flow in the CS, which can force the impurities promptly back to the wall, thereby reducing net erosion relative to gross erosion. Future fusion devices will have high duty cycles which could result in extremely high annual rates of gross erosion; it will therefore be essential to achieve as much prompt, local (re)-deposition of sputtered wall material as possible [5]. For these reasons, it is important to have as physically correct as possible a description of the combined DS and CS for small α, in order to be able to understand and model plasma-surface interactions in magnetic fusion devices, particularly regarding impurity behaviour, and specifically regarding the processes of prompt, local re-deposition of impurities needed to reduce net erosion relative to gross erosion.

We note here that we will not be considering the extreme of $\alpha \to 0$ in this report. It is known [4, 6–11] that for very small $\alpha \lesssim 1^\circ$, the ions reach the wall more quickly than do the electrons, i.e. the reverse of the more familiar situation where the electrons, because of their higher mobility (lower mass) reach the wall faster than the ions, thus charging it negatively. In the latter case, the resulting positive space charge layer in the DS and the electron-repelling potential field in the sheath reduce the electron flux reaching the wall, while accelerating the ion flow, until ambipolar outflow to the electrically floating wall results. However, for $\alpha \lesssim (m_e/m_i)^{1/2}$, which is $\sim 1^\circ$ for a deuterium plasma, the ions reach the wall faster than the electrons because of their larger Larmor radius and as a result a more complex sheath arises. We will not consider this regime here. Such very small α-values are not used in present magnetic fusion devices because of the practical difficulties of achieving the exceptionally high degree of structural alignment required to make effective use of them. This may well change in future devices, however, where there will be strong incentive to use the smallest values of α possible, to reduce the deposited power flux density on the wall, particularly on divertor targets and limiters. A positively charged wall should also experience reduced sputtering. In this report we will be restricting our attention to values of $\sim 1^\circ < \alpha \lesssim 5^\circ$, the range of values generally employed in present magnetic fusion devices and planned for the ITER divertor targets.

The existence of a DS is such a familiar feature of plasma-solid contact that the idea of its disappearance warrants discussion. The present situation does not appear, however, to be essentially different than the disappearance of the DS (a) as the bias potential of a solid surface is moved towards the local plasma potential, or (b) as α is reduced below $\sim 1^\circ$, as just discussed: when a DS no longer seems to be required, e.g. to achieve ambipolar plasma flow to a solid surface, then it is hypothesized to no longer exist. Nevertheless, this has to be treated as a hypothesis until it can be experimentally confirmed.

The CS is quite thin and Chodura, in his original analysis of the CS [2] treated the ions and electrons as collisionless. As discussed in section 10.11 of [3], the neglect of self-collisions is often a good approximation even when self-collisions are in fact frequent, since they do not change the particle content, momentum or average energy of the fluids. We therefore follow Chodura here, although the effect of collisions is of interest, particularly for future devices where very high plasma densities are anticipated at divertor targets, $n_e \sim 10^{21}\,\text{m}^{-3}$ and where the local plasma will also be quite cool, ~few electron volts. This will result in very strong collisionality amongst charged particles, although as noted, that is not very important directly for the CS since momentum and energy are conserved for self-collisions. However, the neutral density will also be high, due to the frequent i–n collisions, $n_{\text{neutral}} \sim n_e$, and neutral frictional drag on the ion flow in the sheaths starts to become important, see [4, 11–13]: for $T = 1$–$10\,\text{eV}$, $n_n = 10^{21}\,\text{m}^{-3}$, $B = 5\,\text{T}$ the charge exchange mfp $\lambda_{cx} \sim 1\,\text{mm}$ while $\rho_{D^+} \sim 0.03$–$0.1\,\text{mm}$ and so collisions are starting to become important. The effect of i–n collisions is to increase $|\Delta\phi_{CS}|$ [4], also $|\Delta\phi_{\text{floating}}|$.

We will also follow Chodura's fluid assumption for the ions [2], although since the scale size of the CS is a few ρ_i, this is an approximation to reality and kinetic treatments are indicated, e.g., [11, 14–16]. We will also make the important simplifying assumption that the electrons are strongly magnetized in both sheaths, and thus their guiding centres follow $\boldsymbol{B}$ all the way to the wall; specifically, we will assume the electrons obey the Boltzmann relation. This should also be relaxed for more quantitative results. In summary, we will use the simplest model, which appears to be capable of

capturing the gross features of the CS. More physically valid quantitative results will require more refined analysis.

The structure of the paper is as follows. Section 2 reviews the Chodura and Riemann analysis for the CS, in order to point out that an important assumption is not necessary which both Chodura and Riemann made, namely that at the exit from the CS the plasma flow speed is sonic in the direction normal to the solid surface, noting in this report that it can instead be subsonic—which would apply to the situation where there is no DS present. Section 3 gives new analysis for the total potential drop across the CS and DS for an electrically floating wall. Section 4 discusses the disappearance of the DS for small α. Section 5 gives the new sheath analysis for the case $\sim 1^\circ < \alpha \lesssim 5^\circ$, where the DS is assumed to no longer exist. Section 6 is discussion and conclusions. Appendix A deals with the special case of supersonic inflow to the CS. Appendix B deals with the special case of a non-floating wall. Appendix C provides convenient numerical expressions for all the sheath quantities of interest, i.e. the plasma density, and electric field vector, etc, as functions of distance in the CS sheath (for small α), or in the combined Chodura plus DS (for large α). The reader who simply wants to use these new solutions for the sheath, can skip the rest of the paper and go directly to appendix C.

2. The fluid analysis of Chodura and Riemann for the collisionless magnetic pre-sheath

Chodura [2] and Riemann [4] use the same fluid model for the collisionless CS. As just noted we review the Chodura and Riemann analysis for the CS, in order to point out that an important assumption is not necessary which both Chodura and Riemann made, namely that at the exit from the CS the plasma flow speed is sonic in the direction normal to the solid surface, noting here that it can instead be subsonic—which would apply to the situation where there is no DS present. Since Riemann's analysis and solutions are more transparent, we follow them here. The geometry is shown in figure 1. The ion particle and momentum equations are

$$\vec{\nabla}\cdot(n_\mathrm{i}\,\vec{v}) = 0, \tag{1}$$

$$m_\mathrm{i}\,\vec{v}\cdot\vec{\nabla}\,\vec{v} = e(\vec{E}+\vec{v}\times\vec{B}) - (\vec{\nabla}\,p_\mathrm{i})/n_\mathrm{i}, \tag{2}$$

where the symbols have their usual meaning, see [4]. For closure the ions are assumed to obey an adiabatic law:

$$\vec{\nabla}\,p_\mathrm{i} = \gamma k T_\mathrm{i}\,\vec{\nabla}\,n_\mathrm{i}. \tag{3}$$

The CS is quasi-neutral and making the usual assumption that the electrons satisfy the Boltzmann relation gives

$$n \equiv n_\mathrm{i} = n_\mathrm{e} = n^{\mathrm{CS\text{-}exit}}\exp[eU/kT_\mathrm{e}], \tag{4}$$

where $n^{\mathrm{CS\text{-}exit}}$ is the density at the *exit* from the CS, i.e. at the entrance to the DS which is taken to be located at $z = 0$, where the electrostatic potential U is assumed to have specified boundary condition $U = 0$. $\vec{E} \equiv -\vec{\nabla}\,U$. Note that this reference location for potential zero differs from the more common one used, which is at the *entrance* to the CS, and which Chodura uses. For clarity, we will use Chodura's symbol

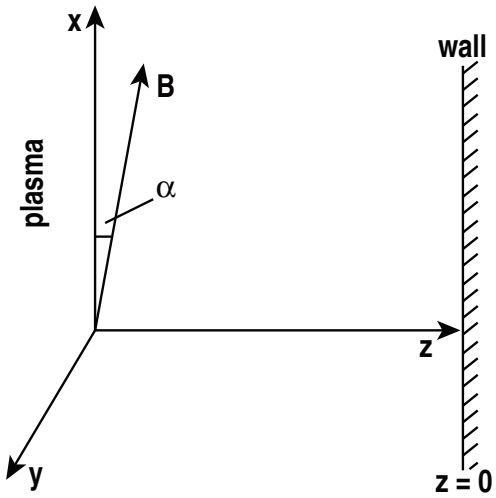

Figure 1. Geometry of the CS model as used in [4]. B is in the x–z plane. The CS is located in the region $z < 0$ with the plasma (SOL) at $z \to -\infty$. The DS is to the right of $z = 0$, immediately in front of the wall, i.e. it is vanishingly thin here.

ϕ for the electrostatic potential with reference zero at the CS entrance, which is assumed to occur far upstream, $z \to -\infty$, i.e. ϕ and U are just mutually off-set. We will find that $\phi(z = 0) < 0$ while at the CS entrance, i.e. in the undisturbed plasma upstream of the CS, we have $U(z \to -\infty) > 0$. Note that the DS is to the right of $z = 0$ in figure 1.

It should be noted that we follow here Riemann [4] and Chodura [2] in assuming the simple Boltzmann relation in the magnetic pre-sheath CS, equation (4). This is an approximation; the electron loss to the solid surface requires the use of a more complex relation between n_e and U involving an error function, see section 4, table 1 of Chodura's analysis for the DS [18]. The error involved approaches a factor of two, with regard to the local electron *density*, as the solid surface is approached; however, fortunately no error is involved with regard to the more important quantity, the electron *flux density* towards the wall, table 1 [18]. Accordingly both Riemann and Chodura applied their analysis based on the simple Boltzmann relation even for small values of α, where it involves an error of almost a factor of 2 with regard to the local electron *density* in the CS near the solid surface. It will be necessary to correct the Riemann/Chodura analysis for $\alpha < \alpha^*$ and the present analysis for $\alpha > \alpha^*$, using the error-function-corrected Boltzmann relation rather than the simple approximate form, to fully assess the magnitude of the error involved here.

Riemann defines

$$\vec{\omega} \equiv e\,\vec{B}/m_\mathrm{i} \tag{5}$$

also the plasma sound speed

$$c_\mathrm{s} \equiv [(kT_\mathrm{e} + \gamma k T_\mathrm{i})/m_\mathrm{i}]^{1/2} \tag{6}$$

and treats it as a constant, thus strictly $\gamma = 1$, isothermal ions are assumed.

Combining equations (1) to (6) gives

$$v_z\frac{\partial v_x}{\partial z} = \omega_z v_y, \tag{7}$$

$$v_z \frac{\partial v_y}{\partial z} = \omega_x v_z - \omega_z v_y, \tag{8}$$

$$v_z \frac{\partial v_z}{\partial z} = -\frac{\omega_x v_y}{1 - c_s^2/v_z^2}. \tag{9}$$

Note that the only spatial variation is in the direction normal to the wall. Riemann assumes that a DS exists at the exit of the CS and therefore that v_z does reach a high enough value, namely $v_z = c_s$, to cause the usual singularity to occur, for instance, in equation (9), it corresponds to the entrance to a net charge layer (DS) and therefore, that the Bohm criterion is satisfied for the ion velocity in the direction normal to the surface there. We will later relax this assumption, allowing v_z to be less than c_s at the exit from the CS.

Thus here ion particle conservation gives

$$n v_z = n_s c_s. \tag{10}$$

Thus

$$n_s \exp[eU/kT_e] v_z = n_s c_s \tag{11}$$

and so

$$U = -\frac{kT_e}{e} \ln\left(\frac{v_z}{c_s}\right), \tag{12}$$

where $n_s \equiv n^{\text{CS-exit}}$. Note that within the CS $v_z/c_s < 1$ therefore, $U > 0$ as already noted.

Riemann introduces dimensionless quantities:

$$\delta \equiv \tan\alpha = \omega_z/\omega_x \tag{13}$$

$$\zeta \equiv z/\rho_i = \omega_x z/c_s, \tag{14}$$

$$u \equiv v_z/c_s, \tag{15}$$

$$v \equiv v_y/c_s, \tag{16}$$

$$w \equiv v_x/c_s, \tag{17}$$

$$\chi \equiv -eU/kT_e. \tag{18}$$

Note that Chodura uses a somewhat different definition for the normalized distance in the perpendicular-to-wall direction (z), e.g. based on length c_s/ω instead of c_s/ω_x where $\omega_x = \omega\cos\alpha$. Equations (7)–(9) can then be rewritten:

$$u w' = \delta\, v, \tag{19}$$

$$u v' = u - \delta\, w, \tag{20}$$

$$u u' = -v/(1 - 1/u^2), \tag{21}$$

where the dash superscript designates the derivative with respect to ζ. Also from equation (12)

$$\chi = \ln u. \tag{22}$$

Riemann obtains a solution by multiplying equations (19)–(21) by w, v and u, respectively, adding and integrating over the CS to obtain an energy equation:

$$u^2 + v^2 + w^2 = 2\ln(u/u_0) + c^2, \tag{23}$$

where c is the integration constant which is related to the initial condition at the entrance to the CS:

for

$$z \to -\infty: \quad u \to u_0 = c\sin\alpha, \quad v \to v_0 = 0, \quad w \to w_0 = c\cos\alpha \tag{24}$$

that is c is the Mach number of the plasma flow in the parallel-to-$\boldsymbol{B}$ direction at the entrance to the CS (CS-ent):

$$c = M^{\text{CS-ent}}_{\parallel\text{-to-}\vec{B}}. \tag{25}$$

Riemann next proves that $c = M^{\text{CS-ent}}_{\parallel\text{-to-}\vec{B}} \geqslant 1$, which is the Chodura condition [2, 4, 17].

The variable v is eliminated from equations (19) and (21) to obtain

$$w = \frac{c + 1/c}{\cos\alpha} - \delta(u + 1/u), \tag{26}$$

where equation (24) was used. Next v from equation (21) and w from equation (26) are substituted into equation (23) to give

$$\left(\frac{1 - u^2}{u}\right)^2 u'^2 = f(u), \tag{27}$$

where

$$f(u) \equiv c^2 + 2\ln(u/u_0) - u^2 - \left[\frac{c + 1/c}{\cos\alpha} - \delta(u + 1/u)\right]^2. \tag{28}$$

The solution for this most basic CS quantity, $u(\zeta)$, is then obtained in the inverse form

$$\zeta(u) = -\int_u^1 \frac{1 - u^2}{u} [f(u)]^{-1/2}\, \mathrm{d}u \tag{29}$$

from which all the other quantities can then be calculated as a function of ζ.

Note Riemann's assumption of the sonic Bohm condition at the exit from the CS, i.e. that $u = 1$ at $z = \zeta = 0$, i.e.

$$M^{\text{CS-exit}}_{\perp\text{-to-wall}} = 1. \tag{30}$$

That is, Riemann assumes that a DS exists starting at the exit from the CS and thus, the upper limit of integration in equation (29) is 1. In this work, we will change this as shown below.

The most general form of the Bohm condition is $M^{\text{DS-exit}}_{\perp\text{-to-wall}} \geqslant 1$, i.e. supersonic influx to the DS is a possible solution. Here this is ruled out because of the simple model used for the CS, which does not permit a continuous (smooth) 'mid-stream' sonic transition: equation (21) only permits a sonic transition singularity at a boundary location; however, see appendix A.

As Riemann notes [4], it is not automatically guaranteed that equation (29) will actually give an asymptotic solution for $u(\zeta)$, i.e. one that will increase from u_0 at $\zeta \to -\infty$, and specifically, it is not automatically guaranteed that $f(u)$ is positive definite for very large (negative) ζ, which is necessary because of the root in equation (29). This therefore provides a fundamental constraint on the solution for the CS. One can readily show from equation (28) that at the CS entrance (at $\zeta \to -\infty$) $f(u_0) = f'(u_0) = 0$ and:

$$f''(u_0) = \frac{2\delta^2}{u_0^2}\left(\frac{1}{u_0^2} - 1\right)(c^2 - 1). \tag{31}$$

Thus, it is necessary that $f''(u_0) \geqslant 0$ and since $u_0 \leqslant u < 1$, then necessarily:

$$c = M^{\text{CS-ent}}_{\parallel\text{-to-}\vec{B}} \geqslant 1, \tag{32}$$

which is the Chodura criterion at the CS entrance. Chodura [2] obtained the same result using a different argument based on the plasma dispersion relation, equation (12) in [2].

It may be noted that the Chodura condition is that $M^{\text{CS-ent}}_{\parallel\text{-to-}\vec{B}}$ be *at least* sonic. In the remainder of the main text we will use the base case assumption of precisely sonic inflow to the CS. The case of supersonic inflow is considered in appendix A.

With the value of c now being known, $c = 1$ here, solutions for all the plasma quantities in the CS can be calculated. The function $f(u)$, equation (28) is now completely specified and so equation (29) can be used to numerically calculate the perpendicular-to-wall speed $u(\zeta) \equiv u(z/\rho_i)$. With c and u known, equation (26) gives the parallel-to-wall speed $w(z/\rho_i)$ and equation (23) gives the $E \times B$ drift speed $v(z/\rho_i)$. Equation (12) gives potential $U(z/\rho_i)$ and equation (4) gives density $n(z/\rho_i)$.

It may be noted that this result, equation (32), does not depend on what happens at the CS *exit* (so long as there is still some ion outflow to the wall). Specifically, it does not require that the Bohm criterion, equation (30), be satisfied there. We will use this fact later in the new analysis developed here, when we relax the Bohm condition at the CS exit.

It is readily shown that equations (19)–(21) give Chodura's master equation for the CS solution, equation (16) in [2]. (Note a typo in that equation: the first term should be V_x^2 not $V_x'^2$.)

Thus from equations (12), (15), (24) and (the sonic form of) (32) we obtain the potential at the CS entrance, i.e. the total potential drop across the CS:

$$U_0 = -\Delta U_{CS} = -\Delta\phi_{CS} = -\frac{kT_e}{e}\ln(\sin\alpha), \tag{33}$$

which, as noted earlier is positive. This is the same result Chodura gives in equation (23) of [2].

3. The total potential drop across the CS and DS for an electrically floating wall

The base case is the electrically floating wall, which we assume in this section. It should be noted, however, that the solid surface is not necessarily floating. It may instead be electrically biased, either intentionally, for instance using an external power supply to bias a Langmuir probe, or naturally e.g. due to thermo-electric effects arising within the plasma. Also, in general, it is only the total assembly of solid surfaces (assumed to be at an equipotential) which float electrically relative to the plasma as a whole and, even if the plasma is assumed to be an equipotential, any individual element of solid surface is unlikely to be floating relative to the local plasma that it is in contact with. In appendix B the case of the non-floating surface is considered.

Assuming the sonic Bohm criterion for the present, the ion flux density normal to, i.e. towards, the wall at the entrance to the DS (exit from the CS) is

$$\Gamma_i^{\perp-\text{wall}} = n_{DS}^{\text{entrance}} c_s, \tag{34}$$

which is also the ion flux density reaching the wall surface.

We will assume that the electrons are very strongly magnetized so that their trajectories follow $\boldsymbol{B}$ all the way to the wall, i.e. the electron Larmor radius ρ_e is small compared with all other system lengths, including the CS and DS thicknesses, $\rho_e \ll \lambda_D$, ρ_i. This assumption considerably simplifies the analysis; however, it is an approximation to reality and the present model is therefore only a first approximation. Thus, the electron parallel-to-$\boldsymbol{B}$ flux density reaching the wall is given by the Boltzmann relation:

$$\Gamma^{\parallel}_{e,\text{wall}} = \tfrac{1}{4} n_{DS}^{\text{entrance}} \bar{c}_e \exp[e\Delta U_{DS}/kT_e], \tag{35}$$

where ΔU_{DS} is the potential drop across the DS (it is negative). Thus, the electron flux density reaching the wall surface is

$$\begin{aligned}\Gamma^{\perp}_{e,\text{wall}} &= \sin\alpha\,\Gamma^{\parallel}_{e,\text{wall}} \\ &= \sin\alpha\,\tfrac{1}{4} n_{DS}^{\text{entrance}} \bar{c}_e \exp[e\Delta U_{DS}/kT_e],\end{aligned} \tag{36}$$

where $\bar{c}_e \equiv (8kT_e/\pi m_e)^{1/2}$.

When the wall surface is electrically floating then the potential drop in the sheath will adjust until there is no net current to the surface, i.e. $\Gamma^{\perp}_{e,\text{wall}} = \Gamma^{\perp}_{i,\text{wall}}$, thus we obtain

$$\frac{e\Delta U_{DS}}{kT_e} = -\ln(\sin\alpha) + 05\ln\left[\left(\frac{2\pi m_e}{m_i}\right)\left(1+\frac{T_i}{T_e}\right)\right]. \tag{37}$$

Combining equations (33) and (37) gives the total potential drop across the combined DS and CS for a floating wall:

$$\begin{aligned}\frac{e\Delta U_{\text{floating}}}{kT_e} &= \frac{e\Delta U_{CS} + e\Delta U_{DS}}{kT_e} \\ &= 0.5\ln\left[\left(\frac{2\pi m_e}{m_i}\right)\left(1+\frac{T_i}{T_e}\right)\right].\end{aligned} \tag{38}$$

Note again that ΔU_{DS}, ΔU_{CS}, and $\Delta U_{\text{floating}}$ are all negative. The expression in equation (38) can be recognized as the standard expression for the potential drop across the DS for a floating wall, which is perpendicular to $\boldsymbol{B}$, $\alpha = 90^\circ$, see [3], i.e. in the case where there is no CS. Thus, the potential of an electrically floating wall is constant, independent of the angle between the wall and $\boldsymbol{B}$.

This was first discovered by Chodura [2] although in [2], he reported it to be only approximately constant based on his kinetic (particle-in-cell, PIC) analysis. The reason that we obtain exact α-independence rather than merely approximate independence is, as explained by Chodura in [18], due to the assumption made here for the electron motion, namely that the electrons are very strongly magnetized, specifically, $\rho_e \ll \lambda_D$ and thus, the electrons follow B even in the DS (they almost always do so in the CS since for most cases of interest $\rho_e \ll \rho_i$). In Chodura's 1982 PIC analysis [2] he assumed $\rho_e \sim \lambda_D$ whereas, in a later study, [8] he assumed $\rho_e \ll \lambda_D$ and in the latter report he shows in fact what appears to be exact α-independence right down to $\alpha \sim 1^\circ$ (figure 2 in [8]). Chodura discusses this in detail in [18], see his figure 11 there and associated discussion.

4. The disappearance of the DS for $\sim 1^\circ < \alpha \lesssim 5^\circ$

We will proceed here assuming the case where the electrons are very strongly magnetized and thus, the total potential drop across the combined CS and DS is precisely constant, independent of α and equal to the standard value, equation (38). We now show that this implies the disappearance of the DS for $\sim 1^\circ < \alpha \lesssim 5^\circ$. We include the first inequality in order to exclude the quite different regime, which occurs for $\alpha \lesssim (m_e/m_i)^{1/2} \sim 0.95^\circ$ for D^+ [4, 6–11]. We again note that this range, $\sim 1^\circ < \alpha \lesssim 5^\circ$ is the one typically used for limiters and divertor targets in magnetic fusion devices.

From equation (37) it is seen that $e\Delta U_{DS}/kT_e = 0$ when $\alpha = \alpha^*$ where

$$\alpha^* \equiv \sin^{-1}\left\{\left[\left(\frac{2\pi m_e}{m_i}\right)\left(1+\frac{T_i}{T_e}\right)\right]^{1/2}\right\}. \qquad (39)$$

Examples: for $T_i = T_e$ then $\alpha^* = 4.746^\circ, 3.354^\circ, 2.999^\circ$ for $m_i = (1, 2, 2.5)m_H$, respectively.

When $\alpha = \alpha^*$, then evidently the DS disappears. What happens for smaller α appears not to have been discussed explicitly in the literature. Chodura does, however, make the following suggestive observations in [18] (note that Chodura uses ψ for the angle between wall and field where $\alpha + \psi = 90^\circ$):

> 'The potential drop in the electrostatic part of the sheath decreases with ψ until for $\psi \to 90^\circ$ the whole potential drop occurs in the magnetic part and the electrostatic part of the sheath completely disappears. The reason for this behaviour is, that for increasing field angles it becomes more difficult for the ions to reach the necessary velocity... for the onset of the electrostatic (Debye) sheath.'

The expression '$\psi \to 90^\circ$' is not quantitative and therefore leaves the exact situation somewhat indefinite. Since, as noted, the apparent disappearance of the DS occurs for angles that are just in the middle of the ones typically used in magnetic fusion devices, we wish to obtain a more precise quantitative result.

The assumption or hypothesis made in the following is that the DS ceases to exist for some specific angle α^* and that only the CS exists for $\sim(m_e/m_i)^{1/2} < \alpha < \alpha^*$. The exact value of $\alpha*$ will depend on the model used, for both the CS and the DS, and for both the ions and the electrons. The present analysis gives the value for α^*, equation (39), for the simplest case: (i) the ions are assumed to have a constant polytropic coefficient γ and to satisfy isothermal fluid modelling in the CS, (ii) the ions are assumed to be collisionless and (iii) the electrons are assumed to be strongly magnetized and to satisfy the simple Boltzmann relation, even in the DS. It will be useful to evaluate α^* based on: (i) kinetic analysis of the ion motion in the CS, (ii) including the effect of collisions, particularly ion–neutral collisions, (iii) electron transport in the DS which is not strongly magnetized, i.e. $\rho_e >$ or $\sim\lambda_D$ and (iv) the error-function-corrected Boltzmann relation. Note also the further assumptions here: (a) a floating wall and (b) the case of sonic inflow to the CS, $M^{\text{CS-ent}}_{\parallel\text{-to-}\vec{B}} = 1$. The last two assumptions are relaxed in appendices A and B to allow for a non-floating wall and supersonic inflow to the CS.

5. A solution for the CS for $\sim 1^\circ < \alpha \lesssim 5^\circ$

For a floating wall with sonic inflow to the CS and for $\sim 1^\circ < \alpha \lesssim 5^\circ$ we assume here that there is no DS, that only the CS exists and that the potential drop across the CS is given by the standard expression, equation (38). For higher values of α the function of the CS is to turn the ion flow (by the CS E-field) so that it changes from being at the sound speed in the parallel-to-$\boldsymbol{B}$ direction at the entrance to the CS to being at the sound speed in the perpendicular-to-wall direction at the CS exit (DS entrance). The total potential drop required in the CS to achieve this is given by equation (33). For a floating wall and for $\sim 1^\circ < \alpha \lesssim 5^\circ$ there is not enough potential drop available across the CS to be able to achieve the full turning of the ion flow. The plasma flow in the direction perpendicular-to-wall at the CS exit therefore, no longer reaches the sound speed, i.e. the Bohm criterion, equation (30), would no longer be satisfied at the DS entrance if there were, in fact, a DS present at the CS exit. However, since there is by the hypothesis made here, no longer any DS present, this does not involve an inconsistency. Instead of the condition at the CS exit being $M^{\text{CS-exit}}_{\perp\text{-to-wall}} = 1$, equation (30), now $M^{\text{CS-exit}}_{\perp\text{-to-wall}}$ is a quantity less than unity that we have to solve for, rather than it being a boundary condition that we have to specify. We next evaluate $M^{\text{CS-exit}}_{\perp\text{-to-wall}}$.

Applying the Boltzmann relation for the potential drop across the CS gives

$$n^{\text{CS-exit}} = n^{\text{CS-ent}} \exp[e\Delta U_{CS}/kT_e] \qquad (40)$$

and since for $\sim 1^\circ < \alpha \lesssim 5^\circ$, $\Delta U_{CS} = \Delta U_{\text{floating}}$, then

$$n^{\text{CS-exit}} = n^{\text{CS-ent}} \exp[e\Delta U_{\text{floating}}/kT_e]. \qquad (41)$$

From ion particle conservation in the CS:

$$n^{\text{CS-ent}} c_s \sin\alpha = M^{\text{CS-exit}}_{\perp\text{-to-wall}} n^{\text{CS-exit}} c_s \qquad (42)$$

and we obtain the result sought:

$$M^{\text{CS-exit}}_{\perp\text{-to-wall}} = \sin\alpha \exp[-e\Delta_{\text{floating}} U/kT_e] \qquad (43)$$

or, using equation (38):

$$M^{\text{CS-exit}}_{\perp\text{-to-wall}} = \left[\left(\frac{2\pi m_e}{m_i}\right)\left(1+\frac{T_i}{T_e}\right)\right]^{-1/2} \sin\alpha. \qquad (44)$$

Some values of $M^{\text{CS-exit}}_{\perp\text{-to-wall}}$ are shown in figure 2. As can be seen, for decreasing α, $M^{\text{CS-exit}}_{\perp\text{-to-wall}}$ decreases, becoming quite subsonic by $\alpha \sim 1^\circ$, where, as noted, a different regime sets in [4, 6–11].

The spatial variation of U, u, etc within the CS is now obtained by a simple modification of the Chodura and Riemann solutions. In equation (29) the upper limit of integration is changed from unity to the value of $M^{\text{CS-exit}}_{\perp\text{-to-wall}} \equiv u^{\text{exit}}$ given by equation (44):

$$\zeta(u) = -\int_u^{M^{\text{CS-exit}}_{\perp\text{-to-wall}}} \frac{1-u^2}{u}[f(u)]^{-1/2}\,du. \qquad (45)$$

For Chodura's solution [2] his boundary condition is $y_0 = \cos\psi \to \cos\psi M^{\text{CS-exit}}_{\perp\text{-to-wall}}$. Note that $f(u)$ is still given by equation (28), and as pointed out above, the value of c is still $c = 1$. Some values of the perpendicular-to-wall Mach number $u(\zeta) \equiv u(z/\rho_i)$ are given in figure 3 for the case of a deuterium plasma.

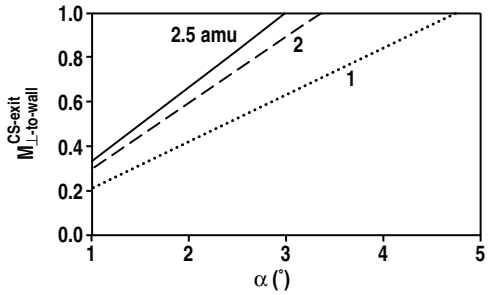

Figure 2. Values of $M^{\text{CS-exit}}_{\perp\text{-to-wall}}(\alpha)$ for $\alpha < \alpha^*$ for several values of the ion mass m_i.

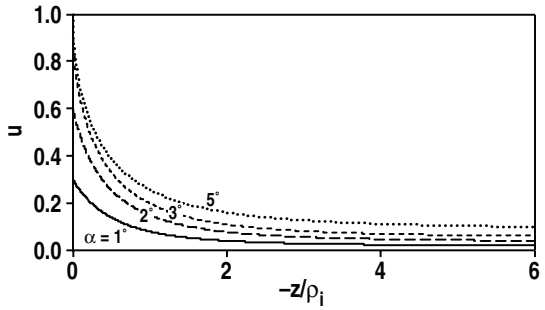

Figure 3. The plasma Mach number in the CS in the perpendicular-to-wall direction, $u[z/\rho_i]$, for several values of α. $m_i = 2$ amu.

6. Discussion and conclusions

Ion sputtering yields are a strong function of the ion impact energy [19] and a significant part of that energy is gained by the ions when they fall through the potential drop across the combined CS and DS. The findings of this report do not alter the long-standing assumption that the total potential drop for an electrically floating wall is given by expressions such as the standard one, equation (38) or equation (A3), independent of the angle α between $\boldsymbol{B}$ and the tangent to the solid surface, provided $\alpha \gtrsim 1^\circ$.

The findings of this report also pertain to the transport of impurity ions in the immediate vicinity of the surfaces of divertor targets and limiters. More specifically, they pertain to the processes involved in prompt, local (re)-deposition of sputtered particles. Because of their high duty cycle, future magnetic fusion devices are likely to experience very high annual rates of gross erosion due to ion sputtering of divertor targets [5]. It is, however, *net* rather than *gross* erosion that mainly matters and when the processes of prompt local re-deposition of sputtered impurities are strong then the net erosion should be much less than the gross erosion.

There are two different processes that can cause sputtered particles to experience prompt, local (re)-deposition, thereby reducing net erosion relative to gross erosion:

(a) Deposition during the first gyro-orbit of the newly ionized sputtered neutral, see discussion in [20],
(b) The forces in the CS, namely the strong electric field and the strong frictional coupling to the fuel ions flowing at high speed towards the target, quickly transporting the ionized impurities back to the target, see e.g. [21].

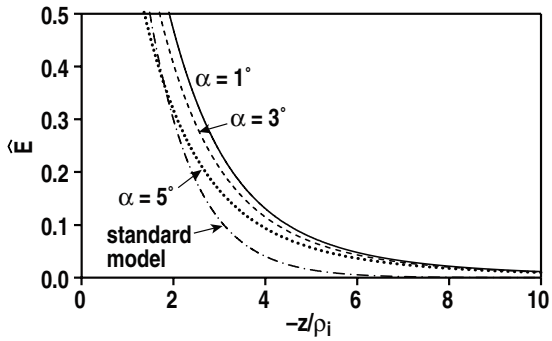

Figure 4. The normalized value of the E_z-field in the CS, $\hat{E}$, as a function of z/ρ_i for several values of α. $m_i = 2$ amu. $E_{\text{actual}} = (kT_e/e\rho_i)\hat{E}$. Also shown is the approximation from the standard model, e.g. [21].

Both of these prompt, local re-deposition processes are included in the codes being used to model the transport of impurities in the edge of tokamaks, such as WBC/REDEP [22], ERO [20, 22, 23], IMPGYRO [24], DIVIMP [25], etc. Typically, these codes use simple approximations to the Chodura solution for the spatial variations and magnitudes of the E-field, and plasma density in the CS. For some situations, these approximations may provide less accurate estimates for the prompt, local re-deposition processes than could be achieved using more complete solutions for these quantities in the CS, such as those derived in this work. We may consider, for example, the approximations explicitly described in [21], which appear to be representative of present impurity codes:

(a) The electrostatic potential in the DS and CS is taken to be given by

$$\phi(z) = \phi_1 \exp[z/2\lambda_D] + \phi_2 \exp[z/\rho_i]. \qquad (46)$$

Thus, $\phi_1(\phi_2)$ is the potential drop across the Debye (Chodura) sheath. It may be noted that the potential in the CS is assumed to vary rather rapidly, $\propto e^{z/\rho_i}$; it will be shown below that the actual Chodura solution gives a more gradual decay of potential, and thus the E-field extends further from the wall. It is also assumed in [21] that $\phi_1 + \phi_2 = \phi_0 = -3kT_e/e$, which this report is in good agreement with, equation (38), including the α-independence. The effect of α on the ratio ϕ_1 to ϕ_2 is included in [21] by specifying a parameter $f_D = 1 - \phi(6\lambda_D)/\phi_0$. Thus, for the value assumed in [21] of $f_D = 0.25$, then $\phi_1 = -0.79kT_e/e$ and $\phi_2 = -2.21kT_e/e$. The resulting spatial variation for the E_z-field ($\equiv d\phi/dz$) are compared with Chodura–Riemann solutions obtained here in figure 4.

(b) As in this report, the spatial variation of plasma density in the CS is assumed to obey the Boltzmann relation; however, since the $\phi(z)$ from equation (46) differs somewhat from the Chodura–Riemann solution, the spatial variation of density differs somewhat also, see comparison in figure 5.

In figure 4 the normalized E_z-field in the CS, $\hat{E} \equiv d\chi/d\zeta$, is compared for $\alpha = 1^\circ$, 3° and 5° for the solutions given by the present analysis and the standard CS approximation, above [21]. The actual E_z-field, $E_{\text{actual}} = (kT_e/e\rho_i)\hat{E}$ can

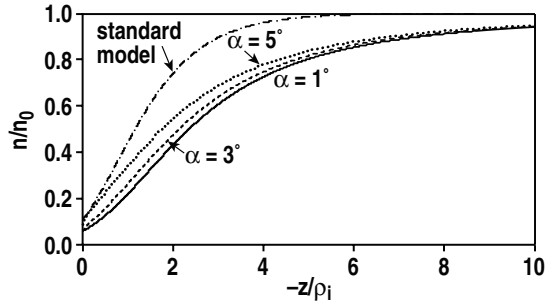

Figure 5. The normalized value of density in the CS, n/n_0, i.e. $n/n(z \to -\infty)$, as a function of z/ρ_i for several values of α. $m_i = 2$ amu. Also shown is the approximation from the standard model, e.g. [21].

be quite strong even at a distance of several ρ_i from the wall; for example, for $T_e = T_i = 10$ eV, D–T ions, and $B = 5$ T then $\rho_i = 1.25 \times 10^{-4}$ m and at $z \sim -4\rho_i$, $\hat{E} \sim 0.1$ and $E_{actual} \sim 10^4$ V m^{-1}, which would exert a strong force on impurity ions, directed back towards the solid surface. As can be seen from figure 4, the E_z-field in the CS obtained from the present analysis extends further from the solid surface than in the standard approximation, which will strengthen the effect of prompt, local re-deposition.

In figure 5 the plasma density in the CS is compared for $\alpha = 1^\circ, 3^\circ$ and 5° for the solutions given by the present analysis and the standard CS approximation, above [21]. As can be seen from figure 5, the density drops more abruptly when approaching the solid surface for the standard approximation than it does for the new CS solutions. This will result in a *weaker* effect of prompt, local re-deposition for the new CS solution for two reasons: (i) the neutral impurities sputtered from the solid surface will penetrate more deeply into the plasma before they are ionized, and (ii) for a given plasma flow velocity, the force of friction dragging the impurity ions back to the solid surface will be reduced because of the lower plasma density (lower collision frequency).

Comparing the present model of the CS with the standard model with regard to the overall effect on the processes of prompt, local re-deposition of impurity particles, since there are off-setting effects it is not obvious what the net effect is and each case has to be individually assessed.

The basic hypothesis made in this report—that for a sufficiently small angle α the DS completely disappears—results from the application of a simple model to the problem, raising the question of whether the DS actually disappears completely in reality. Even for the zero-B case where only the DS exists, it has long been recognized that the assumption that the space in front of the wall can be divided into two distinct regions, namely a quasi-neutral plasma ('pre-sheath') and a net-charge DS, leads to unphysicality: the plasma solution for the pre-sheath has singularities—i.e. unphysical behaviour—at its boundary, e.g., $E \to \infty$. This is interpreted as resulting from the unphysical assumption that the DS is vanishingly thin on the scale-length of the pre-sheath, i.e. $\lambda_D = 0$. Similarly, the solution for the DS assumes $E = 0$ as boundary condition at its entrance, i.e. at the same location where the pre-sheath solution has $E \to \infty$. This major inconsistency can be avoided by not making the assumption of two distinct regions but instead solving for the entire spatial region with a single model; however, then much useful insight is lost. The same situation occurs for the oblique-B case for $\alpha > \alpha^*$ where at the exit from the CS, $E \to \infty$. For $\alpha < \alpha^*$ it is readily shown from the simple model used here that at the exit from the CS, E now remains finite and is of order $kT_e/e\rho_i$, only going to zero as $\alpha \to 0$. While this magnitude of E is generally significantly smaller than E in the DS, which is of order $kT_e/e\lambda_D$, nevertheless it is not zero, which means that—assuming that there is indeed no DS for this case—then E immediately in front of the wall is non-zero. Therefore, if a discontinuity in E is to be avoided, it must be assumed that there is a net (negative) charge on the surface of the wall. The latter, in turn, implies that there *is*, in fact, a net (positive) charge layer immediately in front of the wall. While this net-charge layer is not actually a 'DS' since it does not have the scale-length of the Debye length, it is nevertheless something like a DS, and in any case it is not included in the simple model here. This layer could be called an 'ion Larmor sheath'.

In reality then, for $\alpha < \alpha^*$ the entire drop in potential for a floating wall may not actually occur across the CS, but instead a small part of the drop may occur over a net-charge layer of thickness of order ρ_i. In that case the results obtained in this report are just first approximations to reality, ones that asymptote to the (more) real situation as $\alpha \to 0$. A full resolution of this question will require application of more complex models which relax a number of the simplifying assumptions made here, and which employ the same modelling equations throughout the entire spatial domain of the problem, rather than modelling quasi-neutral and net-charge regions separately.

Acknowledgments

The author wishes to thank Anthony Leonard, Karl Riemann, and Dmitri Ryutov for helpful discussions. He wishes to thank David Tskhakaya for particularly valuable discussions about kinetic analysis of the sheath problem. This work was supported by the U.S. Department of Energy under Cooperative Agreement No. DE-FC02-04ER54698 and the National Sciences and Engineering Research Council of Canada.

Appendix A. The case of supersonic inflow to the CS

The Chodura condition, equation (32), has been analysed in further detail in [17] to clarify why supersonic—not just sonic—plasma flow at the CS entrance is possible, despite the fact that the CS is quasi-neutral. The Bohm criterion, in its marginal form where $M_{\perp\text{-to-wall}}^{DS-ent} = 1$, is associated with a 'gentle entry' into the DS with $\Delta n_e = \Delta n_i$, while $M_{\perp\text{-to-wall}}^{DS-ent} > 1$ corresponds to $\Delta n_e > \Delta n_i$. The CS, in contrast with the DS, is a region of quasi-neutrality and thus, only $\Delta n_e = \Delta n_i$ is permitted. This might appear to prohibit supersonic flow parallel-to-B at the entrance to the CS, which the analysis of Chodura and Riemann has found to be permitted, in fact. This apparent contradiction is resolved [17] by analysing the CS to bring out more explicitly the role played by inertia in the $E \times B$ direction, which confirms that such supersonic flow is permitted.

Table C1. Coefficients for sixth order polynomial fits to the solution for $u(\zeta) \equiv v_z/c_s$, equation (29), for $\alpha > \alpha^*$.

α (°)	Range of validity of ζ	a_6	a_5	a_4	a_3	a_2	a_1	a_0
10	[0, −1]	1.4875E + 1	4.9285E + 1	6.4338E + 1	4.2284E + 1	1.5142E + 1	3.3646E + 0	0.9539
	[−1, −10]	9.1530E − 6	3.2743E − 4	4.7419E − 3	3.5860E − 2	1.5259E − 1	3.6505E − 1	0.6092
5	[0, −1]	1.8831E + 1	6.2159E + 1	8.0793E + 1	5.2830E + 1	1.8806E + 1	4.1153E + 0	0.9438
	[−1, −10]	1.1831E − 5	4.1746E − 4	5.9368E − 3	4.3777E − 2	1.7938E − 1	4.0338E − 1	0.5171
4	[0, −1]	2.0226E + 1	6.6460E + 1	8.5922E + 1	5.5849E + 1	1.9764E + 1	4.3004E + 0	0.9405
	[−1, −10]	1.2295E − 5	4.3389E − 4	6.1613E − 3	4.5250E − 2	1.8391E − 1	4.0715E − 1	0.4908
3	[0, −1]	2.1588E + 1	7.0675E + 1	9.0991E + 1	5.8884E + 1	2.0763E + 1	4.5048E + 0	0.9365
	[−1, −10]	1.3320E − 5	4.6617E − 4	6.5546E − 3	4.7550E − 2	1.9011E − 1	4.1084E − 1	0.4605

Whether the plasma parallel flow speed at the CS entrance is sonic or supersonic depends on conditions *upstream* of the CS entrance, i.e. in the 'pre-sheath', i.e. in the main part of the scrape-off layer (SOL). Assuming that there is a flow stagnation point someplace in the SOL, then for smooth acceleration through a 'mid-stream' sonic point certain conditions have to be satisfied by the plasma fluid in the SOL, see [26]. The most common situation for which a mid-stream sonic transition is expected involves a plasma temperature that decreases rapidly approaching the wall, with a strong ion source, e.g. due to recycle ionization, in the region of rapid temperature decrease [26]. There do not appear to be any direct measurements of plasma flow speed showing a mid-stream sonic transition in a tokamak SOL; however, there is indirect indication of such a transition occurring for just these circumstances [27, 28]. We will not consider the details of mid-stream sonic transitions further here but will simply allow for supersonic inflow at the CS entrance as a possible boundary condition for the sheath problem being considered here.

We now derive an expression for $\Delta U_{\text{floating}}$ for the case of $M^{\text{CS-ent}}_{\|\text{-to-}\vec{B}} > 1$, i.e. the equivalent of equation (38). The parallel ion flux density at the entrance to the CS, which is equal to the parallel ion flux density reaching the wall, is

$$^{\|\text{-to-}B}\text{i}\Gamma^{\text{entrance}}_{\text{CS}} = {}^{\|\text{-to-}B}\text{i}\Gamma^{\text{wall}} = n^{\text{entrance}}_{\text{CS}} M^{\text{CS-ent}}_{\|\text{-to-}\vec{B}} c_s. \quad \text{(A1)}$$

For the electrons, again assuming very strongly magnetized electrons, we have:

$$^{\|\text{-to-}B}\text{e}\Gamma^{\text{wall}} = \tfrac{1}{4} n^{\text{entrance}}_{\text{CS}} \bar{c}_e \exp[e\Delta U_{\text{wall}}/kT_e]. \quad \text{(A2)}$$

For floating conditions $\Delta U_{\text{wall}} = \Delta U_{\text{floating}}$ and equating equations (A1) and (A2) gives:

$$\frac{e\Delta U_{\text{floating}}}{kT_e} = \ln[M^{\text{CS-ent}}_{\|\text{-to-}\vec{B}}] + 0.5 \ln\left[\left(\frac{2\pi m_e}{m_i}\right)\left(1 + \frac{T_i}{T_e}\right)\right]. \quad \text{(A3)}$$

Example: a deuterium plasma, $T_e = T_i$ and $M^{\text{CS-ent}}_{\|\text{-to-}\vec{B}} = 2$, then $e\Delta U_{\text{floating}}/kT_e = -2.15$, compared with -2.84 for $M^{\text{CS-ent}}_{\|\text{-to-}\vec{B}} = 1$. Since the floating potential drop is reduced when $M^{\text{CS-ent}}_{\|\text{-to-}\vec{B}} > 1$, the disappearance of the DS occurs over an even wider range of α values than for $M^{\text{CS-ent}}_{\|\text{-to-}\vec{B}} = 1$. Equating the CS potential drop, equation (33), to $\Delta U_{\text{floating}}$, equation (A3), we now obtain for α^* the result:

$$\alpha^* \equiv \sin^{-1}\left\{M^{\text{CS-ent}}_{\|\text{-to-}\vec{B}}\left[\left(\frac{2\pi m_e}{m_i}\right)\left(1 + \frac{T_i}{T_e}\right)\right]^{1/2}\right\}$$
$$\approx M^{\text{CS-ent}}_{\|\text{-to-}\vec{B}}\left[\left(\frac{2\pi m_e}{m_i}\right)\left(1 + \frac{T_i}{T_e}\right)\right]^{1/2}. \quad \text{(A4)}$$

Example: a deuterium plasma, $T_e = T_i$ and $M^{\text{CS-ent}}_{\|\text{-to-}\vec{B}} = 2$, then $\alpha^* = 6.718$, approximately double the value for $M^{\text{CS-ent}}_{\|\text{-to-}\vec{B}} = 1$.

In section 2 it was argued that for the simple model assumed here for the CS that a supersonic inflow to the DS could not occur but only sonic or subsonic. That, however, also assumed parallel sonic *influx* to the CS. When the latter assumption is relaxed, as here, then supersonic *outflow* from the CS and thus supersonic inflow to the DS is possible. We do not consider this case further here.

Appendix B. The case of a non-floating wall

When the wall is at a negative potential U_{wall} such that $|\Delta U_{\text{wall}}| > |\Delta U_{\text{floating}}|$, where $\Delta U_{\text{floating}}$ is given by equation (38), then both the DS and CS can be expected to exist with

$$U_{\text{wall}} = \Delta U_{\text{CS}} + \Delta U_{\text{DS}} \quad \text{(B1)}$$

$$\text{and from equation (33)} : \Delta U_{\text{CS}} = \frac{kT_e}{e}\ln(\sin\alpha) \quad \text{(B2)}$$

As before, ΔU_{DS} takes up the difference between ΔU_{wall} and ΔU_{CS}. Now $|\Delta U_{\text{DS}}|$ will be greater than for the floating wall.

When the wall is at a less negative potential such that $|\Delta U_{\text{wall}}| < |\Delta U_{\text{floating}}|$ where $\Delta U_{\text{floating}}$ is again given by equation (38), then the DS is assumed to disappear for $\alpha < \alpha^*_{\text{non-fl}}$ where

$$\alpha^*_{\text{non-fl}} = \sin^{-1}\{\exp[e\Delta U_{\text{wall}}/kT_e]\} \quad \text{(B3)}$$

Note that $\alpha^*_{\text{non-fl}} > \alpha^*$ and so the absence of a DS occurs for a larger range of α-values than for a floating wall.

Example: $e\Delta U_{\text{wall}}/kT = -2$, then $\alpha^*_{\text{non-fl}} = 7.78°$, instead of 3.35°.

Appendix C. Numerical expressions for the physical quantities in the CS

In tables C1 and C2, the coefficients a_i, $i = 0$ to 6, are given for sixth order polynomial fits to the numerical solutions obtained here, equations (29) and (45), for the master quantity $u(\zeta) \equiv v_z/c_s$, the normalized flow velocity in the z-direction, where $\zeta \equiv z/\rho_i$, z is the direction perpendicular to the solid surface which is located at $z = 0$, see figure 1. For example, for $\alpha = 10°$ and for $\zeta \in [0, -1]$:

$$u = 14.875\zeta^6 + 49.285\zeta^5 + 64.338\zeta^4 + 42.284\zeta^3$$
$$+15.142\zeta^2 + 3.3646\zeta + 0.9539. \quad \text{(C1)}$$

Table C2. Coefficients for sixth order polynomial fits to the solution for $u(\zeta) \equiv v_z/c_s$, equation (45), for $\alpha < \alpha^*$.

mass	α (°)	range of validity of ζ	a_6	a_5	a_4	a_3	a_2	a_1	a_0
1 amu	4	[0, −1]	6.3069E + 0	2.1751E + 1	3.0084E + 1	2.1648E + 1	9.0952E + 0	2.6901E + 0	0.8324
		[−1, −10]	1.1911E − 5	4.1997E − 4	5.9604E − 3	4.3776E − 2	1.7807E − 1	3.9509E − 1	0.4801
	3	[0, −1]	1.1452E + 0	4.2120E + 0	6.4222E + 0	5.4320E + 0	3.0461E + 0	1.4174E + 0	0.6316
		[−1, −10]	1.0726E − 5	3.7641E − 4	5.3146E − 3	3.8802E − 2	1.5667E − 1	3.4397E − 1	0.4032
	2	[0, −1]	1.8552E − 1	7.4137E − 1	1.2913E + 0	1.3665E + 0	1.0894E + 0	7.5111E − 1	0.4219
		[−1, −10]	7.8798E − 6	2.7680E − 4	3.9107E − 3	2.8554E − 2	1.1518E − 1	2.5205E − 1	0.2899
	1	[0, −1]	2.4947E − 2	1.1302E − 1	2.3963E − 1	3.3765E − 1	3.7430E − 1	3.3265E − 1	0.2110
		[−1, −10]	4.2330E − 6	1.4824E − 4	2.0882E − 3	1.5203E − 2	6.1142E − 2	1.3333E − 1	0.1516
2	3	[0, −1]	1.0929E + 1	3.6682E + 1	4.8949E + 1	3.3501E + 1	1.3033E + 1	3.3949E + 0	0.8720
		[−1, −10]	1.3155E − 5	4.6022E − 4	6.4691E − 3	4.6927E − 2	1.8766E − 1	4.0583E − 1	0.4562
	2	[0, −1]	1.1072E + 0	4.0726E + 0	6.2259E + 0	5.3108E + 0	3.0312E + 0	1.4278E + 0	0.5957
		[−1, −10]	1.1021E − 5	3.8542E − 4	5.4098E − 3	3.9116E − 2	1.5547E − 1	3.3239E − 1	0.3583
	1	[0, −1]	8.1095E − 2	3.4084E − 1	6.4569E − 1	7.7796E − 1	7.2249E − 1	5.4939E − 1	0.2984
		[1, −10]	6.3787E − 6	2.2204E − 4	3.1014E − 3	2.2309E − 2	8.8137E − 2	1.8696E − 1	0.1970
2.5	2	[0, −1]	2.1137E + 0	7.5610E + 0	1.1086E + 1	8.8342E + 0	4.4968E + 0	1.8108E + 0	0.6648
		[−1, −10]	1.2273E − 5	4.2686E − 4	5.9568E − 3	4.2804E − 2	1.6893E − 1	3.5812E − 1	0.3793
	1	[0, −1]	1.2350E − 1	5.0657E − 1	9.2326E − 1	1.0497E + 0	9.0793E − 1	6.4799E − 1	0.3336
		[−1, −10]	7.0756E − 6	2.4679E − 4	3.4507E − 3	2.4814E − 2	9.7805E − 2	2.0631E − 1	0.2134

All the other physical quantities in the CS can then be easily obtained from the values of u. One obtains the flow velocity in the x-direction, $w(\zeta) \equiv v_x/c_s$, where x is the direction parallel to the surface (but not the $E \times B$ direction), see figure 1, from equation (26):

$$w = \frac{2 - (u + 1/u)\sin\alpha}{\cos\alpha}, \tag{C2}$$

where the standard case of $c \equiv M^{\text{CS-ent}}_{\|\text{-to-}\vec{B}} = 1$ has been assumed.

One obtains $v(\zeta) \equiv v_y/c_s$, where y is the direction parallel to the surface and in the $E \times B$ direction, see figure 1, from equation (23):

$$u^2 + v^2 + w^2 = 2\ln(u/\sin\alpha) + 1. \tag{C3}$$

One obtains the normalized electrostatic potential $\chi(\zeta) \equiv -eU/kT_e$ from equation (22):

$$\chi = \ln u \tag{C4}$$

from which the electric field can be found in any direction including the parallel-to-B direction.

The foregoing applies to both $\alpha > \alpha^*$, table C1, and $\alpha < \alpha^*$, table C2.

References

[1] Greenwald M. *et al* 2007 Priorities, gaps and opportunities: towards a long-range strategic plan for magnetic fusion energy *FESAC Report* DOE/SC-102, *FESAC Report* DOE/SC-102 (2007), http://www.science.doe.gov/ofes/FESAC/Oct-2007/FESAC_Planning_Report.pdf

[2] Chodura R. 1982 *Phys. Fluids* **25** 1626

[3] Stangeby P.C. 2000 *The Plasma Boundary of Magnetic Fusion Devices* (Bristol: Institute of Physics) chapter 2

[4] Riemann K.U. 1994 *Phys. Plasma* **1** 552

[5] Stangeby P.C. and Leonard A.W. 2011 *Nucl. Fusion* **51** 063001

[6] Daybelge U. and Bein B. 1981 *Phys. Fluids* **24** 1190

[7] Behnel J. 1985 *PhD Thesis* Ruhr-Universitat Bochum *Report* 85-02-118 SFB 162

[8] Chodura R. 1992 *Europhys. Conf. Abstracts* **16c** (Pt.II) 871

[9] Cohen R.H. and Ryutov D.D. 1995 *Phys. Plasmas* **2** 4118

[10] Cohen R.H. and Ryutov D.D. 1995 *Phys. Plasmas* **2** 2011

[11] Tskhakaya D. and Kuhn S. 2003 *J. Nucl. Mater.* **313–316** 119

[12] Hua T.Q. and Brooks J.N. 1994 *Phys. Plasmas* **1** 3607

[13] Zimmermann T.M.G., Coppins M. and Allen J.E. 2008 *Phys. Plasmas* **15** 072301

[14] Schmitz H., Riemann K.U. and Daube T.H. 1996 *Phys. Plasmas* **3** 2486

[15] Daube T.H., Riemann K.U. and Schmitz H. 1998 *Phys. Plasmas* **5** 117

[16] Daube T.H. and Riemann K.U. 1999 *Phys. Plasmas* **6** 2409

[17] Stangeby P.C. 1995 *Phys. Plasmas* **2** 702

[18] Chodura R. 1986 *Physics of Plasma–Wall Interactions in Controlled Fusion* (*NATO ASI Series B: Physics* vol 131) ed D.E. Post and R. Behrisch (New York: Plenum)

[19] Eckstein W. 2002 Calculated sputtering, reflection and range values *Report* IPP 9/32

[20] Naujoks D. *et al* 1996 *Nucl. Fusion* **36** 671

[21] Brooks J.N. 1990 *Phys. Fluids* B **2** 1858

[22] Naujoks D. 1997 *Nucl. Fusion* **37** 1193

[23] Kirschner A. *et al* 2009 *Phys. Scr.* **T138** 014011

[24] Hyodo I. *et al* 2003 *J. Nucl. Mater.* **313–316** 1183

[25] Stangeby P.C. 2000 *The Plasma Boundary of Magnetic Fusion Devices* (Bristol: Institute of Physics) chapter 6

[26] Stangeby P.C. 2000 *The Plasma Boundary of Magnetic Fusion Devices* (Bristol: Institute of Physics) chapter 14

[27] Leonard A.W. *et al* 1997 *Phys. Rev. Lett.* **78** 4769

[28] Leonard A.W. *et al* 1998 *Phys. Plasmas* **5** 1736